6

Power Quality Improvement in Distribution Network with Renewable Energy Sources using DSTATCOM with Battery Energy Storage System

The power quality disturbances associated with the grid integrated RE sources such as solar and wind energy systems have been successfully detected using the Stockwell's transform as detailed in the previous chapters. This chapter presents power quality improvement in the presence of grid disturbances, wind energy penetration, solar energy penetration and simultaneous operations of wind as well as solar energy penetration using distribution static compensator (DSTATCOM) with battery energy storage system.

6.1 INTRODUCTION

The power quality disturbances detected in the power system network can effectively be mitigated with the help of a distribution static compensator (DSTATCOM). The distribution static compensator is a voltage source converter (VSC) based device usually supported by short-time energy stored in the dc link capacitor. It can compensate for reactive power, load unbalancing, voltage variations and current harmonics in the distribution network [Shukla et al., 2008]. Performance of the DSTATCOM depends on estimation of active and reactive powers, harmonic currents, and control algorithm used for estimation of reference currents [Arya et al., 2014a]. The control techniques of DSTATCOM like instantaneous $p-q$ theory, synchronous reference frame theory (SRF), Modified synchronous reference frame theory (*MSRF*), instantaneous symmetrical control theory, and average unit power factor theory (AUPF) have been reported in the literature [Sahu and Mahapatra, 2014]. The battery energy storage system (BESS) connected to the dc bus in parallel with dc link capacitor improves the dynamic performance of the system such as frequency and voltage regulation. The battery energy storage system provides the additional capacity of DSTATCOM for load balancing, reactive power compensation, harmonic current elimination, and also functions as un-interruptible power supply (UPS) [Singh and Niwas, 2012]. Implementation of the DSTATCOM, addressing power quality improvement, for specific applications such as isolated wind power generation, residential low voltage network, load compensation, isolated asynchronous generator, standalone solar photovoltaic system and water pumping system has been reported in the literature. However, very less number of articles are available for implementation of DSTATCOM at grid level addressing PQ improvement specifically with renewable energy sources. Ghosh *et al.* [Ghosh and Joshi, 2004], proposed a DSTATCOM with battery energy storage system for voltage regulation in the mini custom power park. The voltage flicker mitigation of electric arc welder has been achieved using DSTATCOM with BESS and reported in [Virulkar and Aware, 2008]. Improvement of the load voltage for a constant speed wind energy system supplying the power to inductive load has been achieved with the help of Fuzzy logic based control of DSTATCOM in [Bhattacharjee et al., 2012]. Alka *et al.* [Singh et al., 2012], proposed the DSTATCOM for compensation of linear and non-linear loads in both steady state and dynamic conditions. The self-charging control technique of DSTATCOM for mitigation of voltage sag, swell and momentary interruption has been proposed in [Woo et al., 2001]. The power quality improvement with wind energy system has been presented by the authors in [Yuvaraj et al., 2011].

This chapter proposes the implementation of DSTATCOM with battery energy storage system in the three phase balanced distribution network addressing PQ issues. Synchronous reference frame theory based control algorithm is used for the control of DSTATCOM. The power quality improvement during disturbances in the grid due to feeder tripping, feeder re-closing, load switching, voltage sags and swells have been investigated. Power quality events with wind energy operations such as outage of wind generator, grid synchronization of wind generator and wind speed variations have also been investigated. The proposed DSTATCOM is also implemented for the improvement of power quality in distribution utility network in the presence of solar PV system during the events such as grid synchronization of solar PV system, outage of solar PV system and variation in solar insolation. Finally, the proposed DSTATCOM is also used for PQ improvement in the hybrid power system.

6.2 PROPOSED TEST SYSTEM

The test system described in the Section 5.2 is used for the study of mitigation of PQ disturbances in the distribution system caused due to grid disturbances, wind generator operations, wind speed variations, solar PV system operations and variations in solar insolation. The test system is modified to incorporate the DSTATCOM with battery energy storage system (BESS), wind generator, solar PV system and load (L) as shown in Fig. 6.1. In the proposed study DSTATCOM is connected at bus 632 of the test system. The wind generator and solar PV system are connected at bus 680 through transformers XWG and XSPV using the circuit breakers CB2 and CB3 respectively. A load (L) comprising of $500kW$ and $500kVAr$ is also connected to the bus 680 with the help of circuit breaker (CB1). The technical data of wind generator and solar PV system as described in the Section 5.2 are used for this study.

6.3 MATHEMATICAL MODELLING OF PROPOSED DSTATCOM AND OPERATIONAL PRINCIPLE

The three-leg topology of three-phase three-wire DSTATCOM with battery bank proposed for power quality improvement and load compensation in the distribution test feeder is shown in Fig. 6.2. The point of common coupling (PCC) is selected between the utility grid and the IEEE-13 bus test feeder for connection of proposed DSTATCOM. This DSTATCOM consists of AC inductor, ripple filter, dc link capacitor, battery bank, and three-leg voltage source converter. Insulated gate bipolar transistors (IGBTs) with anti-parallel diodes are used as switches of the VSC. The combination of six switches in the Fig. 6.2 represents the voltage source converter. The design of various components of DSTATCOM are detailed in the following subsections.

6.3.1 DC Link Capacitor

The capacitor connected on dc side of the VSC is known as dc link capacitor (C_{dc}). Design of this capacitor depends on the ability of VSC to regulate voltage during transients [Kumar and Mishra, 2013]. DC link capacitor injects or absorbs active power during transients to maintain the load demand. The value of this capacitor depends on the minimum and maximum battery voltages and instantaneous energy available to the DSTATCOM during transients [Singh et al., 2014c]-[Rohilla and Pal, 2013]. The value of dc link capacitor is given by equation (6.1) based on the principle of energy conservation [Labeeb and Lathika, 2011].

$$\frac{1}{2}C_{dc}[V_{dc}^2 - V_{dc1}^2] = 3VaIt \tag{6.1}$$

where V_{dc1} is minimum voltage level of dc bus; V is the phase voltage; t is the time by which dc bus voltage is to be recovered, and I is the phase current. Taking, $V_{dc1} = 6970V$, V_{dc}=$7000V$, $V = 2.402kV$, $I = 486A$, $t = 350\mu s$ and $a = 1.2$, the calculated value of dc link capacitor is approximately $7000\mu F$. The design value of dc link capacitor (C_{dc}) used in this study is $10000\mu F$.

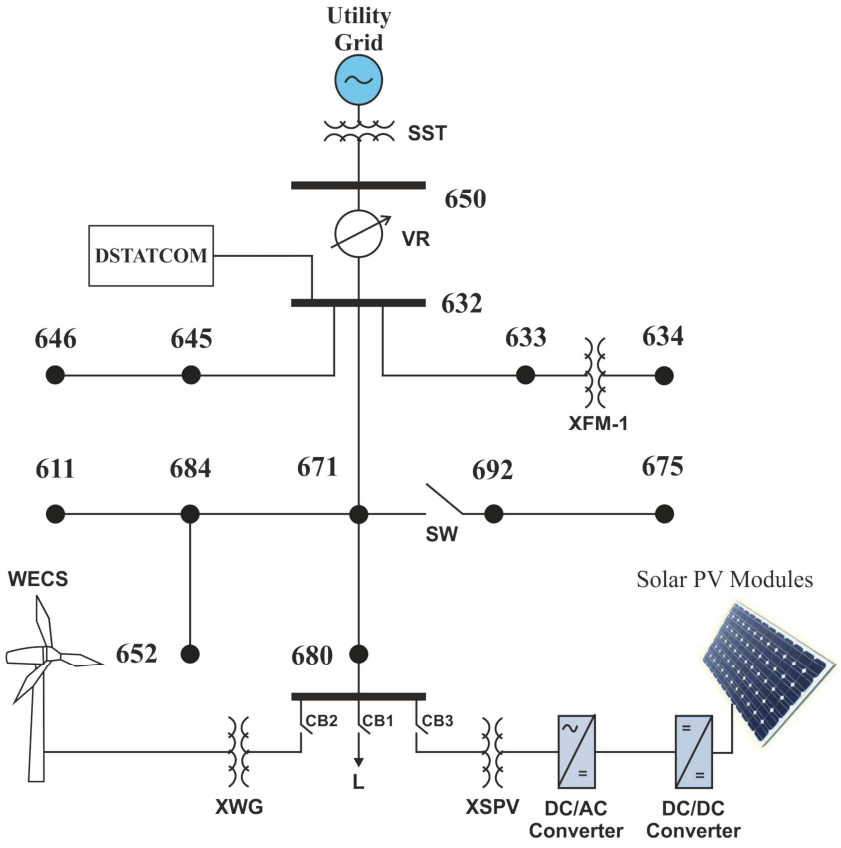

Figure 6.1 : Modified IEEE-13 bus test system incorporated with DSTATCOM and RE sources

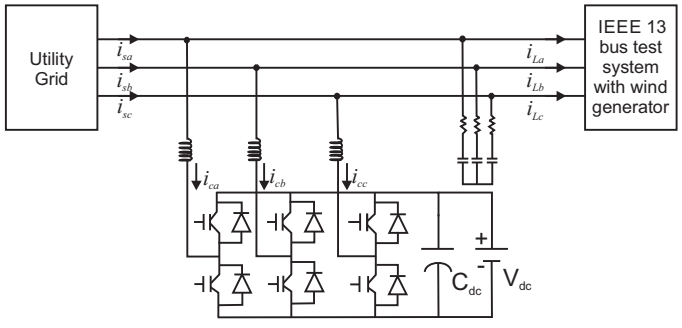

Figure 6.2 : Proposed DSTATCOM with BESS

6.3.2 AC Inductor

The interfacing inductor (L_f) is connected on ac side of three-leg VSC between VSC and PCC. For successful operation of the DSTATCOM, voltage drop across the interfacing inductor

should not be greater than 8% [Singh et al., 2014b]. The design value of L_f is given by the following relation [Singh et al., 2008b].

$$L_f = \frac{\sqrt{3}mV_{dc}}{12af_sI_{cr(p-p)}} \tag{6.2}$$

where f_s is switching frequency; V_{dc} is dc bus voltage; a is overload factor and $I_{cr(p-p)}$ is peak to peak current ripple. Taking, $I_{cr(p-p)} = 25\%$, $V_{dc} = 7000V$, $f_s = 10kHz$, $a = 1.2$, and m=1, the L_f is calculated to be $3.4mH$. A design value of $4.0mH$ is selected in this study.

6.3.3 Ripple Filter

A high pass first order filter consisting of series resistor (R_f) and capacitor (C_f) tuned at half the switching frequency is utilized as the ripple filter. It is connected in shunt to the system and used to filter out noise from the voltage at PCC [Singh et al., 2008a]. Time constant of the ripple filter is very small compared to the fundamental time constant (T) and should satisfy the following condition [Singh et al., 2009]

$$R_fC_f \ll T/10 \tag{6.3}$$

$R_f = 0.1\Omega$ and $C_f = 10\mu F$ are used as design values in this study.

6.3.4 Battery Bank

A battery bank (V_{dc}) is connected in parallel with the dc link capacitor as shown in Fig. 6.2. For satisfactory operation of the DSTATCOM, dc link voltage should be more than twice the peak value of phase voltage of the ac system [Singh and Sharma, 2012]. Hence, the dc link voltage opted is given by the following relation [Singh et al., 2014d].

$$V_{dc} = \frac{2\sqrt{2}V_{LL}}{\sqrt{3}m} \tag{6.4}$$

where m is modulation index and V_{LL} is ac line to line voltage at PCC. Here, calculated value of V_{dc} is 6793 V for $m = 1$ and $V_{LL} = 4.16kV$. The battery voltage in this study is kept at 7000 V.

6.3.5 Principle of Operation

Principle of operation of the proposed DSTATCOM is based on the real and reactive powers that can be exchanged between the PCC and inverter output of the DSTATCOM. [Mitra and Venayagamoorthy, 2010]. The active power (P) and reactive power (Q) exchange between DSTATCOM and PCC are given by the following relations

$$P = \frac{V_{PCC}V_C \sin\alpha_{pcc}}{X} \tag{6.5}$$

$$Q = \frac{V_{PCC}(V_{PCC} - V_C\cos\alpha_{pcc})}{X} \tag{6.6}$$

where α_{pcc} is the angle between the bus and inverter output voltages, V_C is magnitude of inverter output voltage, V_{PCC} is magnitude of PCC voltage, and X is the reactance between the PCC and inverter output terminals.

6.4 PROPOSED DSTATCOM CONTROLLER

The controller for VSC of the DSTATCOM generates reference source currents using SRF theory with carrier based pulse width modulation (PWM) technique [Zaveri et al., 2011]-[Singh and Solanki, 2009] as shown in Fig. 6.3. SRF theory based controller involves the sensing of line voltages and load currents. The Clark's transformation is used to convert three-phase instantaneous load currents (I_{La}, I_{Lb}, I_{Lc}) into two-phase currents (I_α, I_β) in stationary frame using the following relation.

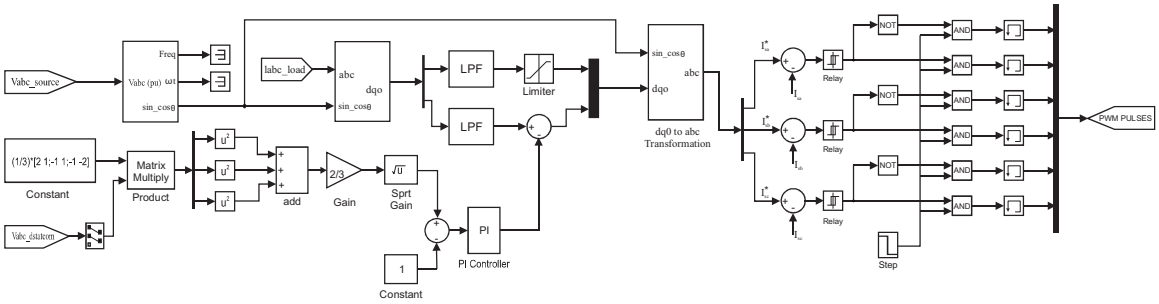

Figure 6.3 : Proposed SRF based control technique of DSTATCOM

$$\begin{bmatrix} I_\alpha \\ I_\beta \end{bmatrix} = \sqrt{\frac{2}{3}} \begin{bmatrix} 1 & -\frac{1}{2} & -\frac{1}{2} \\ 1 & \frac{\sqrt{3}}{2} & -\frac{\sqrt{3}}{2} \end{bmatrix} \begin{bmatrix} I_{La} \\ I_{Lb} \\ I_{Lc} \end{bmatrix} \tag{6.7}$$

The park's transformation is used to convert currents in stationary frame to synchronously rotating frame known as $d-q$ components (I_d, I_q) as given by the following relation.

$$\begin{bmatrix} I_d \\ I_q \end{bmatrix} = \begin{bmatrix} \cos\theta & \sin\theta \\ -\sin\theta & \cos\theta \end{bmatrix} \begin{bmatrix} I_\alpha \\ I_\beta \end{bmatrix} \tag{6.8}$$

where θ is transformation angle. The $\cos\theta$ and $\sin\theta$ are obtained from phase voltages using Phase locked loop (PLL) technique. The $d-q$ components of current are passed through the low pass filter to extract the dc components (I_{ddc}, I_{qdc}). The active power component of fundamental reference source current (I^*_{ddc}) is generated by limiting the active power component between 85% to 100% of the rated load in the IEEE-13 bus network without considering the renewable power generation. DSTATCOM supplies real power when load becomes more than rated load (100%) and it absorbs the same when load becomes less than 85% of the rated value. In the presence of renewable power generation, the power drawn by the test system is less than 85% of rated value which results in the power absorbed by the DSTATCOM.

The phase voltages at PCC are calculated from any two line voltages by the following relation.

$$\begin{bmatrix} V_A \\ V_B \\ V_C \end{bmatrix} = \frac{1}{3} \begin{bmatrix} 2 & 1 \\ -1 & 1 \\ -1 & -2 \end{bmatrix} \begin{bmatrix} V_{AB} \\ V_{BC} \end{bmatrix} \tag{6.9}$$

Phase voltages are used to calculate the amplitude of instantaneous terminal voltage at PCC using the following relation

$$V_t = \sqrt{\frac{2}{3}(V_A^2 + V_B^2 + V_C^2)} \tag{6.10}$$

The voltage error input to the PI controller is given as

$$V_{error} = V_{tref} - V_t \tag{6.11}$$

where V_{tref} is the reference terminal voltage which is taken as 1 pu in this study.

Reactive power component of fundamental reference source current (I^*_{qdc}) is generated by subtracting reactive power component from output of the PI controller. These active and reactive power components of fundamental reference source currents are used to generate three-phase fundamental reference source currents ($I^*_{sa}, I^*_{sb}, I^*_{sc}$).

Active and reactive power components of the fundamental reference source currents are used to generate the three-phase reference source currents using inverse Park's and Clark's transformation as given in equations (6.12) and (6.13) respectively.

$$\begin{bmatrix} I^*_{\alpha dc} \\ I^*_{\beta dc} \end{bmatrix} = \begin{bmatrix} \cos\theta & \sin\theta \\ -\sin\theta & \cos\theta \end{bmatrix} \begin{bmatrix} I^*_{ddc} \\ I^*_{qdc} \end{bmatrix} \tag{6.12}$$

$$\begin{bmatrix} I^*_{sa} \\ I^*_{sb} \\ I^*_{sc} \end{bmatrix} = \sqrt{\frac{2}{3}} \begin{bmatrix} 1 & 0 \\ -\frac{1}{2} & \frac{\sqrt{3}}{2} \\ -\frac{1}{2} & -\frac{\sqrt{3}}{2} \end{bmatrix} \begin{bmatrix} I^*_{\alpha dc} \\ I^*_{\beta dc} \end{bmatrix} \tag{6.13}$$

The reference source currents obtained in equation (6.13) are compared with the source currents (I_{sa}, I_{sb}, I_{sc}) captured at PCC and current error signal is generated. This error signal is used to generate the pulse width modulation (PWM) signals by hysteresis PWM controller which are utilized as gate signal for the IGBT of voltage source converter.

6.5 PROPOSED PQ IMPROVEMENT STRATEGY

The DSTATCOM with BESS is connected on the bus 632 of the IEEE-13 bus test feeder. A load comprising of 500 kW and 500 kVAr is connected to the bus 680 with the help of a circuit breaker to study the PQ events with the grid disturbances. A solar PV system of capacity $500kW$ and DFIG based wind energy system with capacity $1.5MW$ are connected to the bus 680 using circuit breakers. The voltage at bus 632 and current flowing between the utility grid and test feeder are continuously tracked with the help of SRF theory based controller and an error signal is generated based on the reference parameters. This error signal is utilized to generate the PWM signals for gating the IGBTs of the VSC which controls the active and reactive power flow between the PCC and DSTATCOM. The error signal will be generated depending on variations in the standard values of voltage and current. Hence, the SRF theory based control of DSTATCOM with BESS can effectively be utilized for PQ improvement at grid level under various case studies of grid disturbances, synchronization/outage of wind generator and solar PV system.

6.6 MITIGATION OF POWER QUALITY DISTURBANCES USING DSTATCOM: CASE STUDIES

This section details simulation results of various case studies. The power injected by the utility grid into the IEEE-13 bus test system and consumed by the load are considered as positive. The DSTATCOM is considered as source of active and reactive powers if power flows out of the DSTATCOM whereas it acts as load if power is absorbed. Real power supplied by the DSTATCOM (P_d) can be expressed in terms of utility grid power P_s and load power P_l by the following relation

$$P_d = P_l - P_s \tag{6.14}$$

The P_d is considered positive for power flows from DSTATCOM to the load and vice versa. Similarly, the reactive power supplied by the DSTATCOM (Q_{dd}) can be expressed in terms of reactive powers of utility grid Q_s and load Q_l by the relation

$$Q_{dd} = Q_l - Q_s \tag{6.15}$$

For reactive power flow from DSTATCOM to the grid, Q_{dd} is positive and vice-versa.

There is no exchange of active and reactive powers by the DSTATCOM in the absence of solar PV system and wind energy system. Power exchange is observed during the events of grid synchronization and outage of solar PV system and wind generator. Power quality investigations have been carried out during above mentioned events. Active power, reactive power and harmonic compensations have been analysed in all the events. Voltage has been captured at bus 632 for the proposed study. The simulations results and discussion are detailed in the following subsections.

6.6.1 Grid Disturbances

This section presents the investigations of PQ events made in the events such as feeder tripping and re-closing, voltage sag, swell, and load switching with and without DSTATCOM. Active power, reactive power and harmonic compensations have been analysed in these investigations.

(a) Feeder Tripping and Re-closing

The circuit breaker between the nodes 671 and 692 is opened at 0.33 second to simulate the feeder tripping and re-closed at 0.67 second. The rms value of voltage at bus 632, active and reactive powers flow into the test feeder from utility grid without DSTATCOM in the system are shown in Fig. 6.4. Tripping of this feeder reduces 1013 kW of active power, 613 kVAr of inductive reactive power and 600 kVAr of capacitive reactive power. It can be observed that total active and reactive powers consumed by the loads in the distribution network are supplied by the utility grid which is verified by overlapping of curves of P_s over P_l in Fig. 6.4 (b) and Q_s over Q_l in Fig. 6.4 (c). Transients in the voltage at the instants of feeder tripping and re-closing are observed having the peak magnitude of 50 V and 20 V respectively. Voltage in this duration has increased by 5 V (approximately). Significant transients in the active and reactive powers have been observed during feeder re-closing as shown in Fig. 6.4 (b) and (c) respectively.

Fig. 6.5 illustrates the transients associated with feeder tripping and re-closing in the presence of DSTATCOM. The DSTATCOM absorbs active and reactive powers during this period. Power supplied by the utility grid is more compared to the power consumed by the load. Thus, the surplus power is used for battery energy storage and capacitor charging. Hence, the voltage during this period remains the same. However, transients are observed in the rms value of voltage at the instants of tripping and re-closing of the feeder. Peak magnitude of the transient voltages at the time of feeder tripping and re-closing are observed as 10 V and 7 V respectively. Thus, a reduction of 80% at the time of feeder tripping and 65% at the time of feeder re-closing in the peak values of transients have been observed in the presence of DSTATCOM. Transients in the active and reactive powers during feeder re-closing have been reduced significantly by the use of DSTATCOM

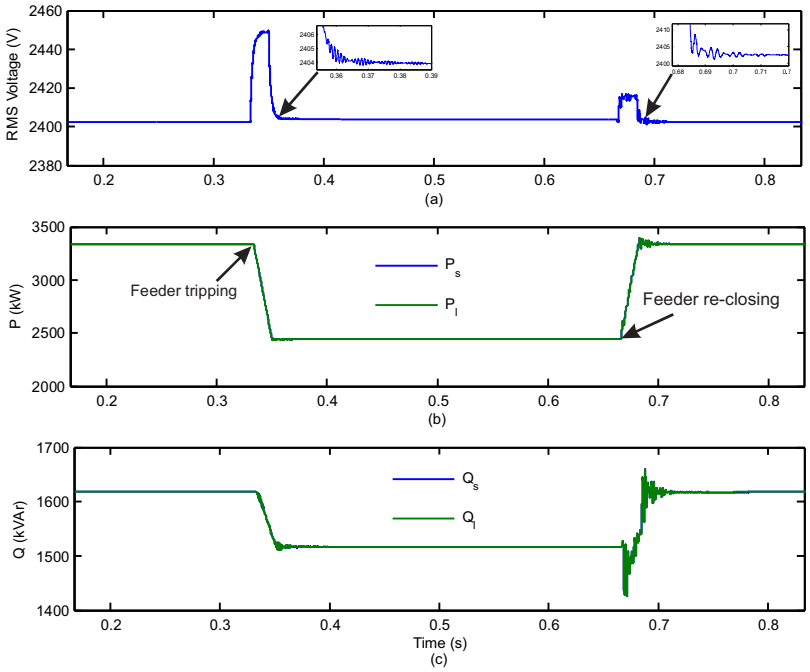

Figure 6.4 : Feeder tripping and re-closing without DSTATCOM in the network (a) RMS voltage at bus 632 (b) Active powers flow and (c) Reactive powers flow

as shown in Fig. 6.5 (b) and (c) respectively. These transients slightly decrease the active power supplied by the DSTATCOM for short duration after feeder re-closing as observed in Fig. 6.5 (b).

Fast Fourier transform (FFT) analysis of the voltage signal at bus 632 is carried out. The total harmonic distortion of voltage (THDv) in the absence of DSTATCOM is observed as 0.087%, whereas the same is observed as 0.031% in the presence of DSTATCOM. Thus, 65% reduction in THDv has been achieved by the application of the DSTATCOM.

(b) Load Switching

A load comprising of 500 kW active and 500 kVAr reactive powers is switched on at bus 680 by connecting the circuit breaker at 0.33 second and switched off at 0.67 second. The rms value of voltage at bus 632, active and reactive powers flow in the test feeder from utility grid for load switching without DSTATCOM are shown in Fig. 6.6. It can be observed that additional active and reactive powers demanded by the load are supplied from the utility grid which is verified by overlapping of curves of P_s over P_l in Fig. 6.6 (b) and Q_s over Q_l in Fig. 6.6 (c). Voltage sag is observed due to decrease in voltage magnitude from the value of 2402 V to 2397 V (0.208% voltage sag of magnitude 5 V) at the time of switching on the load and restored to original value after the load is switched off. Transients of low magnitude are observed in the voltage at the time of load switching as shown in Fig. 6.6 (a).

Fig. 6.7 depicts the rms value of voltage at bus 632, active and reactive powers flow into the test feeder from utility grid for load switching with DSTATCOM. It can be observed that DSTATCOM compensated the active and reactive powers during this period. From Fig. 6.7 (a), it can be observed that voltage sags to 2400 V (0.08325% voltage sag with magnitude of 2 V) in the presence of DSTATCOM. Magnitude of voltage sag is decreased as compared to the case of without

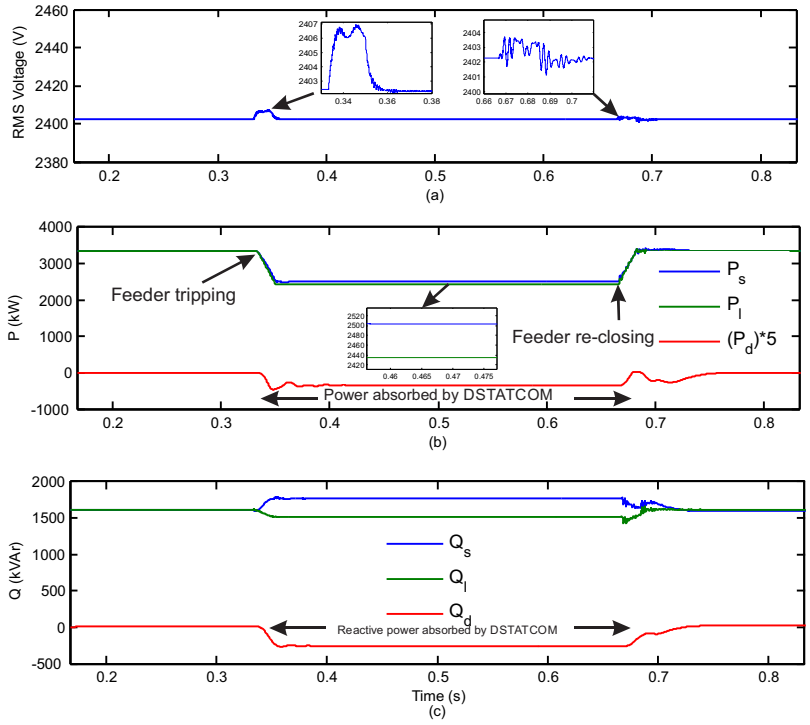

Figure 6.5 : Feeder tripping and re-closing with DSTATCOM in the network (a) RMS voltage at bus 632 (b) Active powers flow and (c) Reactive powers flow

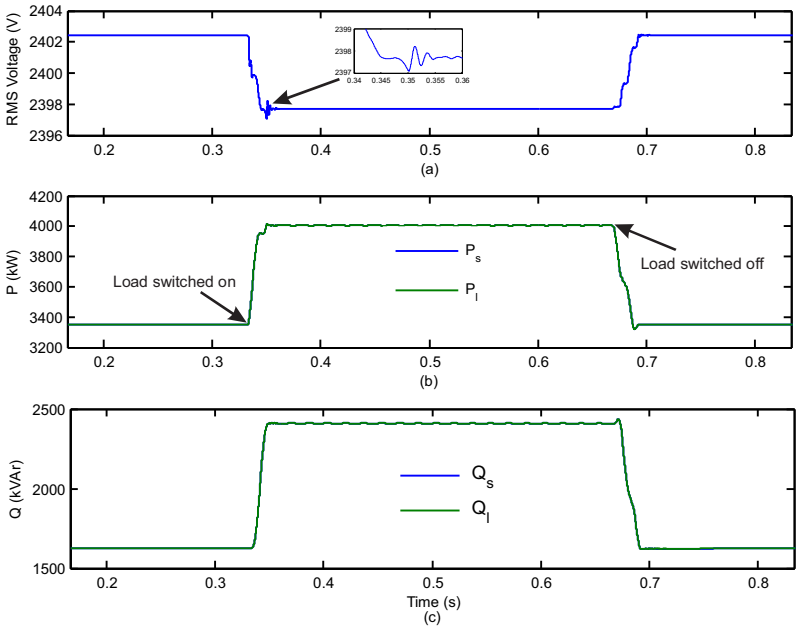

Figure 6.6 : Load switching without DSTATCOM in the network (a) RMS voltage at bus 632 (b) Active powers flow and (c) Reactive powers flow

DSTATCOM. Hence, a reduction of 60% in the voltage sag has been achieved by the application of DSTATCOM during load switching. Magnitude of the voltage transients have also decreased with the compensation provided by DSTATCOM.

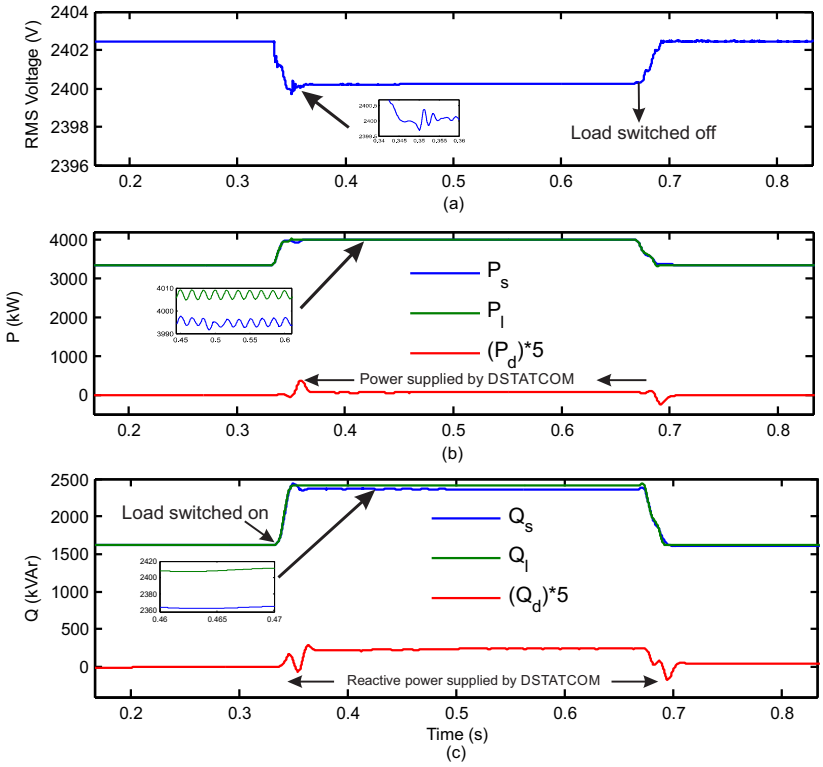

Figure 6.7 : Load switching with DSTATCOM in the network (a) RMS voltage at bus 632 (b) Active powers flow and (c) Reactive powers flow

The THDv of voltage measured at bus 632 during load switching without DSTATCOM is observed as 0.042%, whereas the same is observed as 0.020% in the presence of DSTATCOM. Thus, 52.38% reduction in THDv has been achieved.

(c) Voltage Sag and Swell

The voltage sag is simulated by reducing the magnitude of utility grid voltage from 2402 V to 2282 V (5% voltage sag) at 0.2 second and again restoring at 0.4 second. The voltage swell is simulated by increasing the voltage magnitude to 2522 V (5% voltage swell) at 0.6 second and restoring the voltage at 0.8 second. The simulated voltage sag and swell are shown in Fig. 6.8 (a). Voltage sag and swell with DSTATCOM and reactive powers flow are shown in Fig. 6.8 (b) and (c) respectively. It can be observed that in the presence of DSTATCOM, 2.5% of voltage sag is recovered. Similarly, DSTATCOM reduces the swell by 2.5%. Thus, a reduction of 50% in the magnitude of voltage sag and swell has been observed in the presence of DSTATCOM. This improvement in the voltage sag and swell has been observed due to the reactive power exchange between the DSTATCOM and utility grid as shown in Fig. 6.8 (c). Transients in the voltage, active and reactive powers have not been observed during the voltage sags and swells.

The THDv of voltage at bus 632 in the absence of DSTATCOM is observed as 0.027%, whereas the same is observed as 0.011% in the presence of DSTATCOM. Thus, 59.26% reduction in THDv has been achieved by the application of DSTATCOM in the test feeder. Comparative study of THDv in the events of grid disturbances under investigation has been tabulated in Table 6.1.

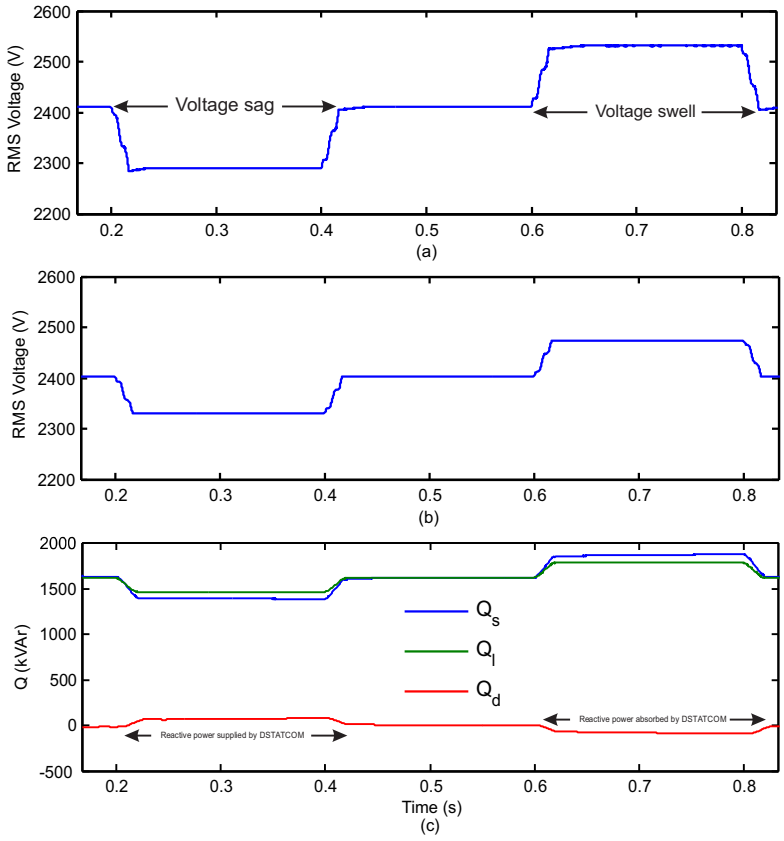

Figure 6.8 : Voltage sag and swell (a) Voltage without DSTATCOM (b) Voltage with DSTATCOM and (c) Reactive powers flow during voltage sag and swell

Table 6.1 : THD of Voltage with Grid Disturbances

Case studies	THD_v (%)		Improvement in THD_v (%)
	Without DSTATCOM	With DSTATCOM	
Feeder tripping and re-closing	0.087	0.031	65.00
Load switching	0.042	0.020	52.38
Voltage sag and swell	0.027	0.011	59.26

6.6.2 Wind Energy Penetration

The power quality investigations have been made in the events of wind operations such as outage of wind generator, grid synchronization of wind generator and wind speed variations with DSTATCOM in the power network. Active power, reactive power and harmonic compensations have been analysed in all these events. Results are presented in the following subsections.

(a) Grid Synchronization of Wind Generator

The circuit breaker used to integrate wind generator is switched on at 1.67 second to simulate the grid synchronization of wind generator. Fig. 6.9 (a) and (b) represent the voltages at bus 632 with and without DSTATCOM. The active and reactive powers flow with DSTATCOM are shown in Fig. 6.9 (c) and (d) respectively. It can be observed that the voltage due to wind energy

penetration has increased from 2402.5 V to 2409 V without DSTATCOM (0.27% increase). This is caused due to available capacitive reactive power compensation with DFIG. In the presence of DSTATCOM wind penetration has increased the voltage to 2407 V (0.18% increase). Hence, improvement in voltage profile has been achieved by the use of DSTATCOM. The peak magnitude of voltage during synchronization has been observed as 12 V and 9 V with and without DSTATCOM as shown in Fig. 6.9 (a) and (b) respectively. Hence, DSTATCOM reduces the peak value of transient voltages through 25%. Thus, an overall improvement in the transient and steady state voltages of bus 632 has been observed with the use of DSTATCOM. The active and reactive powers injected in to the network under investigation are reduced due to available local generation of wind. Hence, the surplus active and reactive powers are absorbed by the DSTATCOM during this period. Power transients are observed for a duration of 0.4 second with active power and 0.8 second with reactive power as depicted in Fig. 6.9 (c) and (d) respectively. However, short duration transient of high magnitude available with active power is observed due to inrush current drawn by the DFIG of wind energy conversion system (WECS).

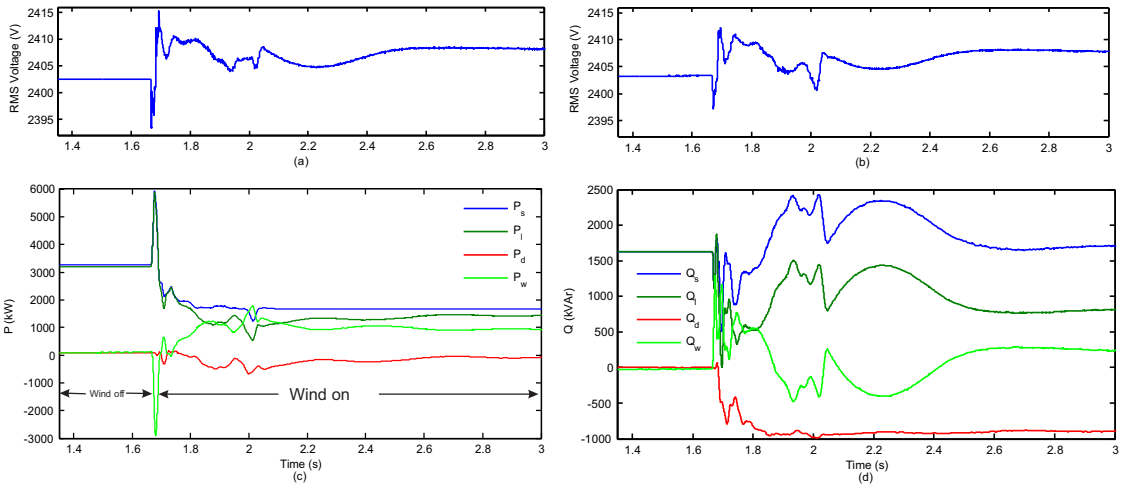

Figure 6.9 : Wind synchronization (a) Voltage without DSTATCOM (b) Voltage with DSTATCOM (c) Active powers flow with DSTATCOM (d) Reactive powers flow with DSTATCOM

FFT analysis of voltage signal at bus 632 is carried out. THDv of bus voltage in the absence of DSTATCOM is observed as 0.07%. In the presence of DSTATCOM the value of THDv almost reduces to zero. Hence, no harmonic distortion is observed with DSTATCOM in the network.

(b) Outage of Wind Generator

Wind outage is simulated by opening the circuit breaker connecting the wind generator on bus 680 at 1.67 second. The rms value of voltages at bus 632 with and without DSTATCOM are shown in Fig. 6.10 (a) and (b) respectively. The active and reactive powers flow with DSTATCOM are shown in the Fig. 6.10 (c) and (d) respectively. It can be observed that the voltage due to wind outage reduces from 2407.5 V to 2402.5 V without DSTATCOM (reduction by 5 V). In the presence of DSTATCOM wind outage has decreased the bus voltage to 2404 V (reduction by 2.5 V) as shown in Fig. 6.10 (a) and (b) respectively. Thus, improvement in the voltage profile by 50% has been observed by the use of DSTATCOM. Transients in the voltage during wind outage have also been reduced significantly by the use of DSTATCOM. Hence, the transient with peak value of 1 V observed without DSTATCOM as shown in Fig. 6.10 (a) at the moment of switching out the wind generator has not been observed in the presence of DSTATCOM as described in Fig. 6.10 (b). From Fig. 6.10 (c) and (d), it can be observed that the surplus active and reactive powers available with wind generation are used to store energy in the BESS and charging the capacitor. However, the

power supplied by the wind and power taken by the DSTATCOM reduces to zero at the moment of wind outage. Low frequency transients are observed in the real power during wind outage. Reactive power is absorbed by the DSTATCOM when the wind generation is available due to the capacitive compensation of DFIG for supplying the reactive power.

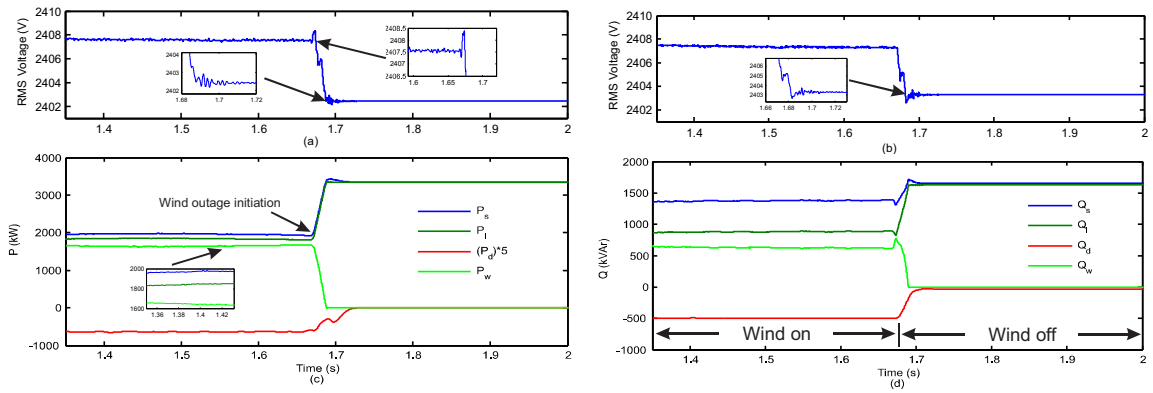

Figure 6.10 : Wind outage (a) Voltage without DSTATCOM (b) Voltage with DSTATCOM (c) Active powers flow with DSTATCOM (d) Reactive powers flow with DSTATCOM

The FFT analysis of voltage signal at bus 632 is carried out. The THDv without the use of DSTATCOM is observed as 0.84%, whereas in the presence of DSTATCOM, the THDv reduces to 0.44%. Thus, a reduction of 47.62% in the THDv has been achieved.

(c) Wind Speed Variation

The variations of wind speed are simulated as shown in Fig. 6.11, where two changes of low magnitude and high magnitude are investigated. The wind speed abruptly decreases to 10 m/s at 1.6 second and restores at 1.8 second. In the second change, the wind speed decreases to 4 m/s between 2.15 second to 2.7 second.

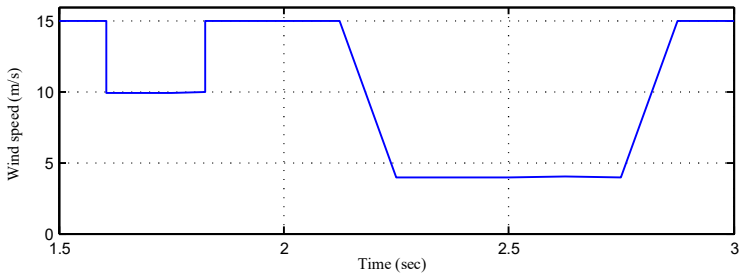

Figure 6.11 : Wind speed variation

Fig. 6.12 (a) and (b), represent the voltages at bus 632 with and without DSTATCOM respectively. The active and reactive powers flow with DSTATCOM are shown in Fig. 6.12 (c) and (d) respectively. It can be observed that transients are not observed in the voltage during wind speed variations. However, the magnitude of voltage decreases by 2 V with second change in the wind speed and same is compensated by 50% in the presence of DSTATCOM. From Fig. 6.12 (c), it can be depicted that slight power variations are observed for small change in the wind speed and variations of high magnitude are observed with high speed wind gusts. Hence, the power demanded by load is supplied by utility grid and DSTATCOM during this period. The reactive

power is not affected by the small wind speed variations. However, the large changes in the wind speed affect the reactive power flow. The reactive power demanded by the load with low wind speed intervals is supplied by the utility grid and DSTATCOM. Hence, it can be observed that DSTATCOM effectively compensates the active and reactive power variations due to changes in the wind speed.

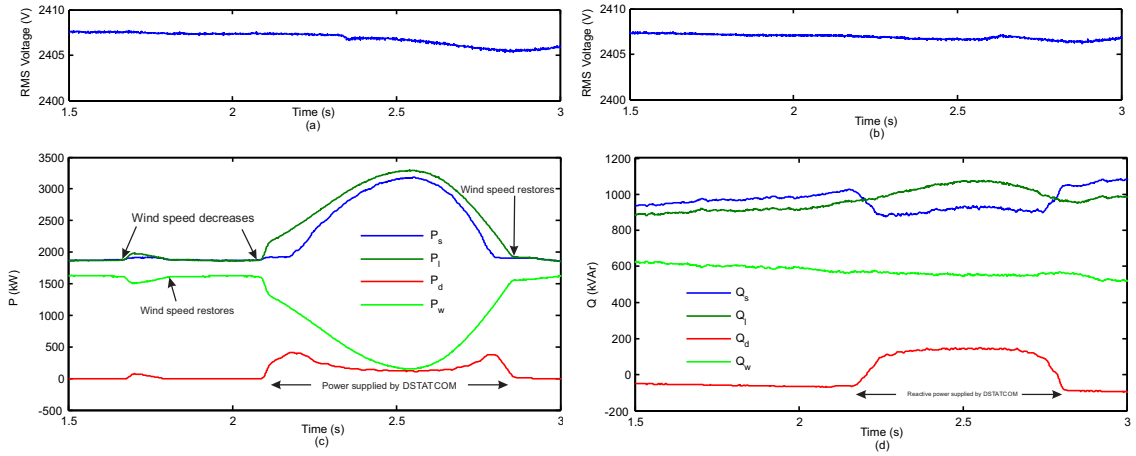

Figure 6.12 : Wind speed variations (a) Voltage without DSTATCOM (b) Voltage with DSTATCOM (c) Active powers flow with DSTATCOM (d) Reactive powers flow with DSTATCOM

The THDv of bus voltage in the absence of DSTATCOM is observed as 0.83%, whereas the same reduces to 0.42% by the application of DSTATCOM. Thus, a reduction of 48.19% in the value of THDv has been achieved by the use of DSTATCOM. The comparative study of THDv with wind energy penetration is provided in Table 6.2. It can be observed that DSTATCOM is highly effective in reduction of harmonics due to wind energy penetration into the distribution network.

Table 6.2 : THD of Voltage with Wind Energy Penetration

Case studies	THD_v (%) at bus 632		Improvement in THD_v (%)
	Without DSTATCOM	With DSTATCOM	
Outage of wind generator	0.84	0.44	47.62
Grid synchronization of wind generator	0.07	0	100
Wind speed variation	0.83	0.42	48.19

6.6.3 Solar Energy Penetration

The power quality investigations have been carried out during the events of grid synchronization and outage of solar PV system as well as sudden change in solar insolation. There is no exchange of active and reactive powers by the DSTATCOM in the absence of solar PV energy system. Power exchange is observed during the above mentioned events. The active power, reactive power and harmonic compensations have been analysed in all the events. Voltage has been captured at bus 632 for the proposed study. The results are presented in the following subsections.

(a) Outage of solar PV Plant

The outage of solar PV system is simulated by opening the circuit breaker connecting the solar PV system on the bus 680 at 0.47 s. The rms value of voltage at bus 632 without and with

DSTATCOM are shown in Fig. 6.13 (a) and (b) respectively. The active and reactive powers flow with DSTATCOM are shown in Fig. 6.13 (c) and (d) respectively. It can be observed that the voltage at the time of solar PV outage rises to 2312 V from 2295 V and then decreases to minimum voltage of 2265 V without DSTATCOM and finally it settles at 2270 V during the time solar PV is switched off as shown in Fig. 6.13 (a). In the presence of DSTATCOM with solar PV outage, the voltage at the time of solar PV outage rises to 2305 V from 2395 V and then it reduces to 2270 V during the time solar PV is switched off as shown in Fig. 6.13 (b). Thus, improvement in the voltage peak by 41% has been achieved by the use of DSTATCOM. Transient in the voltage during solar PV outage have also been reduced significantly by the use of DSTATCOM as shown in Fig. 6.13 (a) and (b). From Fig. 6.13 (c), it can be observed that the surplus active power available with solar PV generation is used to store energy in the BESS and charging the capacitor. However, the active power supplied by the solar PV system and power taken by the DSTATCOM reduces to zero at the moment of solar PV outage. Low frequency power variations are observed in the active power during outage of solar PV system. From Fig. 6.13 (d), it has been observed that the surplus reactive power available has been absorbed by the DSTATCOM to charge the capacitor whereas the reactive power is not supplied by the solar PV system because it generates the dc power. After the solar PV sytem outage, the reactive power is not absorbed by the DSTATCOM. However, a transient event in the reactive power is observed due to the outage of solar PV system. This is due to the reactive compensation provided to the solar PV system by the use of capacitor.

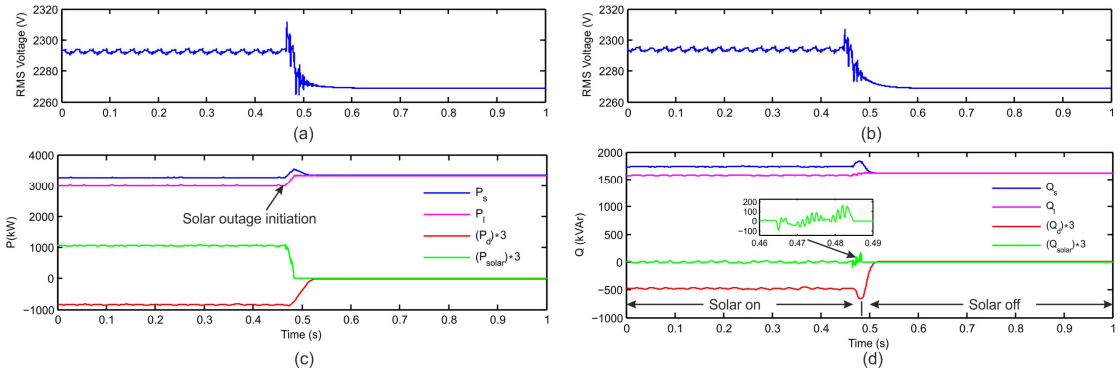

Figure 6.13 : Solar PV outage (a) Voltage without DSTATCOM, (b) Voltage with DSTATCOM, (c) Active powers flow with DSTATCOM and (d) Reactive powers flow with DSTATCOM

The FFT analysis of voltage signal at bus 632 is carried out. The total harmonic distortions in voltage (THD_v) without the use of DSTATCOM is observed as 5.50%, whereas in the presence of DSTATCOM, the THD_v reduces to 3.73%. Thus, a reduction of 37.63% in the value of THD_v has been achieved by the use of DSTATCOM with BESS.

(b) Grid Synchronization of solar PV plant

The circuit breaker used to integrate the solar PV system is switched on at 0.52 s to simulate the grid synchronization of solar PV system. Fig. 6.14 (a) and (b) respectively represent the voltages at bus 632 without and with DSTATCOM. Active and reactive powers flow with DSTATCOM are shown in Fig. 6.14 (c) and (d) respectively. It can be observed that maximum voltage deviation during the event of grid synchronization of solar PV system is 10 V (0.4402%). In the presence of DSTATCOM, the grid synchronization of solar PV system has deviated the voltage by 7 V (0.3083%). Hence, improvement (by 29.96%) in the voltage deviation has been achieved by the use of DSTATCOM. Active and reactive powers injected into the network by the substation transformer are reduced due to the available local solar PV generation. Hence, the surplus active and reactive powers are absorbed by the DSTATCOM during this period. Power transients are observed with active and reactive powers for a duration of 0.1 s as depicted in Fig. 6.14 (c) and (d)

respectively.

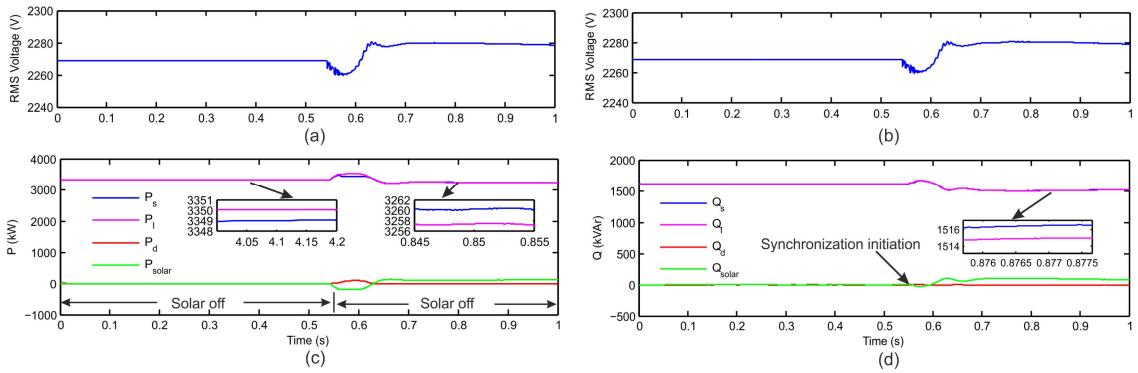

Figure 6.14 : Grid synchronization of solar PV system (a) Voltage without DSTATCOM, (b) Voltage with DSTATCOM, (c) Active powers flow with DSTATCOM and (d) Reactive powers flow with DSTATCOM

FFT analysis of voltage signal at bus 632 is carried out. The THD_v without the use of DSTATCOM is observed as 2.59%. In the presence of DSTATCOM the value of THD_v reduces to 0.20%. Thus, an improvement in the value of THD_v has been achieved by 92.28%.

(c) Variation in Solar Insolation

The solar insolation has been reduced abruptly from $1000w/m^2$ to $600w/m^2$ at 0.5 s. Fig. 6.15 (a) and (b), represent voltages at bus 632 without and with DSTATCOM respectively. Active and reactive powers flow with DSTATCOM are shown in Fig. 6.15 (c) and (d) respectively. It can be observed that transients in the voltage have been observed for long duration without the use of DSTATCOM whereas these transients are limited to 0.15 s in the presence of DSTATCOM with BESS as shown in the Fig. 6.15 (a) and (b). Hence, reduction in the voltage transients has been observed by the use of DSTATCOM. From Fig. 6.15 (c) and (d), it can be depicted that variations are observed in the active and reactive powers for a duration of 0.12 s following the abrupt change in the solar insolation. From Fig. 6.15 (c), it can be observed that power generated by the solar PV system is decreased due to the reduction in solar insolation and consequently the power absorbed by the DTSTACOM with BESS is also reduced. Active and reactive powers absorbed by the DTSTACOM have been reduced with decrease in the solar insolation. Hence, it can be observed that DSTATCOM with BESS effectively compensates the active and reactive powers due to abrupt change in the solar insolation.

FFT analysis of voltage signal at bus 632 during the event of sudden change in solar insolation is carried out. The THD_v without the use of DSTATCOM is observed as 6.62%. In the presence of DSTATCOM with BESS, the value of THD_v reduces to 3.73%. Thus, an improvement in the value of THD_v has been achieved by 43.65%. The comparative study of THD_v with solar PV system based energy penetration into the utility grid is provided in the Table 6.3. It can be observed that DSTATCOM with BESS is highly effective in reduction of harmonics due to solar PV energy penetration into distribution network of the power system.

6.6.4 Hybrid Power System

The power quality investigations have been carried out during the events of grid synchronization and outage of solar PV system and wind generator in the presence of each of other and simultaneous events. There is no exchange of active and reactive powers by the DSTATCOM in absence of the solar PV system and wind energy system. Power exchange is observed during the

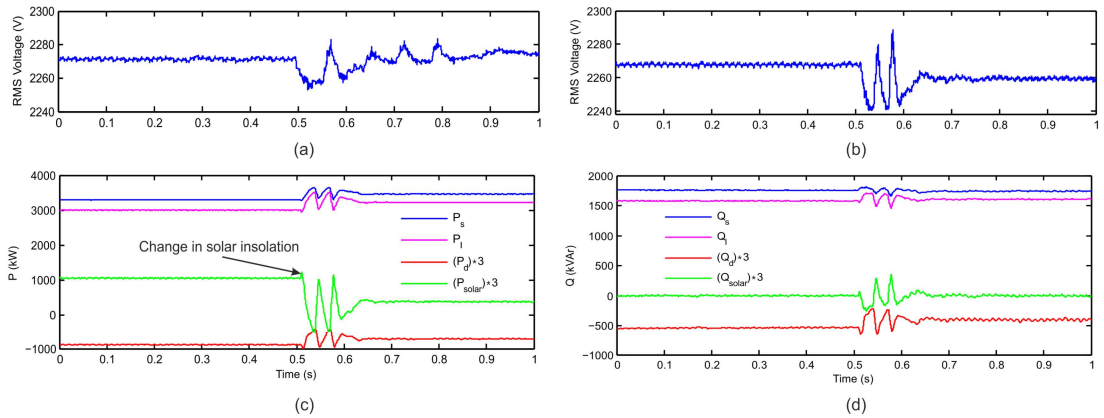

Figure 6.15 : Abrupt change in solar insolation (a) Voltage without DSTATCOM, (b) Voltage with DSTATCOM, (c) Active powers flow with DSTATCOM and (d) Reactive powers flow with DSTATCOM

Table 6.3 : THD of Voltage with Solar Energy Penetration

Case studies	THD_v (%) at bus 632		Improvement in THD_v (%)
	Without DSTATCOM	With DSTATCOM	
Outage of solar PV generator	5.50	3.43	37.63
Grid synchronization of solar PV system	2.59	0.20	92.28
Change in solar insolation	6.62	3.73	43.65

above mentioned events. The active power, reactive power and harmonic compensations have been analysed in all the events. Voltage has been captured at bus 632 for the proposed study. Results are presented in the following subsections.

(a) Outage of Wind Generator in the Presence of Solar PV System

The outage of wind generator in the presence of solar PV system is simulated by opening the circuit breaker connecting the wind generator on the bus 680 at 0.50 s. The rms value of voltage at bus 632 without and with DSTATCOM are shown in Fig. 6.16 (a) and (b) respectively. Active and reactive powers flow with DSTATCOM are shown in Fig. 6.16 (c) and (d) respectively. It can be observed that voltage has decreased from 2408.5 V to 2404 V (reduction by 0.187%) without DSTATCOM. In the presence of DSTATCOM wind outage has decreased the voltage from 2406.5 V to 2404.5 V (reduction by 0.083%). Hence, improvement in voltage profile by 55.61% has been achieved by the use of DSTATCOM. From the Fig. 6.16 (c) and (d), it can be observed that the surplus active and reactive powers available with wind and solar PV generation are used to store energy in the BESS and charging the dc-link capacitor. However, the active and reactive powers supplied by the wind generator reduces to zero at the moment of wind outage whereas the DSTATCOM supplies the active and reactive powers to meet out the load demand in the absence of wind power generation. Low magnitude variations are observed in the active and reactive powers supplied by the solar PV system at the moment of wind outage. Hence, wind outage also affects output power of the solar PV system for short duration.

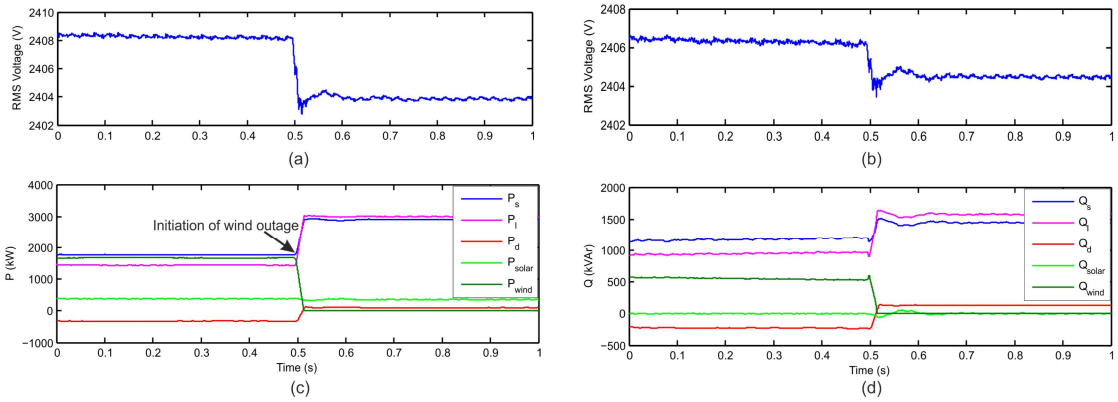

Figure 6.16 : Outage of wind generator in the presence of solar PV system (a) Voltage without DSTATCOM (b) Voltage in the presence of DSTATCOM (c) Active powers flow with DSTATCOM and (d) Reactive powers flow with DSTATCOM

Voltage signal at bus 632 is analysed using FFT. The total harmonic distortions in voltage (THD_v) of bus voltage in the absence of DSTATCOM is observed as 0.3192%. In the presence of DSTATCOM with BESS the value of THD_v reduces to 0.1608%. Thus, an improvement in THD_v by 49.62% is achieved with the use of DSTATCOM.

(b) Outage of Solar PV System in the Presence of Wind Generator

The outage of solar PV system in the presence of wind generator is simulated by opening the circuit breaker connecting the solar PV system on the bus 680 at 0.50 s. The rms value of voltage at bus 632 without and with DSTATCOM are shown in Fig. 6.17 (a) and (b) respectively. The active and reactive powers flow with DSTATCOM are presented in Fig. 6.17 (c) and (d) respectively. It can be observed that outage of solar PV system has increased the voltage by 1.5 V with a transient peak to peak value of 1.5 V. In the presence of DSTATCOM solar PV outage has not changed the voltage magnitude and transient peak value has also reduced to 0.75 V. Hence, improvement in voltage profile by 100% has been observed by the use of DSTATCOM and transient peak value has improved by 50%. From Fig. 6.17 (c) and (d), it can be observed that the surplus active and reactive powers available with wind and solar PV generation are used to store energy in the BESS and charging the dc-link capacitor. The active and reactive powers supplied by the solar PV system reduces to zero at the moment of solar PV outage. Active power taken by the DSTATCOM reduces to zero and reactive power taken is reduced due to solar PV outage. Low frequency transients are observed in the reactive powers supplied by the wind generator and solar PV system due to the solar PV outage. Low frequency power transients are also observed in the power supplied by the utility grid and wind generator. Hence, solar PV outage also affects the output power of the wind generator for short duration.

FFT analysis of voltage signal at bus 632 is carried out. The THD_v without the use of DSTATCOM is observed as 0.2565%, whereas in the presence of DSTATCOM, the THD_v is reduced to 0.1318%. Hence, a reduction of 48.62% in the THD_v has been achieved by the use of DSTATCOM with the outage of solar PV system in the presence of wind generator.

(c) Simultaneous Outage of Solar PV System and Wind Generator

The simultaneous outage of solar PV system and wind generator is simulated by opening the circuit breakers connecting these generators on the bus 680 at 0.50 s. The rms value of voltage at bus 632 without and with DSTATCOM are shown in Fig. 6.18 (a) and (b) respectively. The active

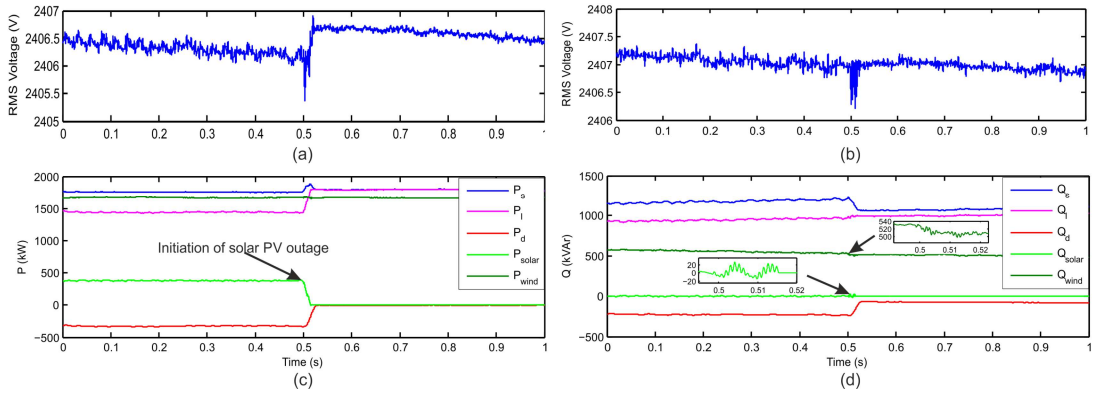

Figure 6.17 : Outage of solar PV system in the presence of wind generator (a) Voltage without DSTATCOM (b) Voltage in the presence of DSTATCOM (c) Active powers flow with DSTATCOM and (d) Reactive powers flow with DSTATCOM

and reactive powers flow with DSTATCOM are presented in Fig. 6.18 (c) and (d) respectively. It can be observed that simultaneous outage of solar PV system and wind generator has decreased the voltage from 2407.5 to 2402 V (reduction by 0.228%) without DSTATCOM. In the presence of DSTATCOM, the outage has decreased the voltage from 2406.5 V to 2403.5 V (0.124% decrease). Hence, improvement in voltage profile by 45.61% has been achieved by the use of DSTATCOM. From the Fig. 6.18 (c) and (d), it can be observed that the surplus active and reactive powers available with wind and solar PV generation are used to store energy in the BESS and charging the dc-link capacitor. However, the active and reactive powers supplied by the wind and solar PV generators reduced to zero at the moment of outage of the generators. The DSTATCOM supplies the active and reactive powers to meet out the load demand after the outage of solar PV system and wind power generation. Low frequency transients are observed in the reactive powers supplied by the solar PV system due to outage event.

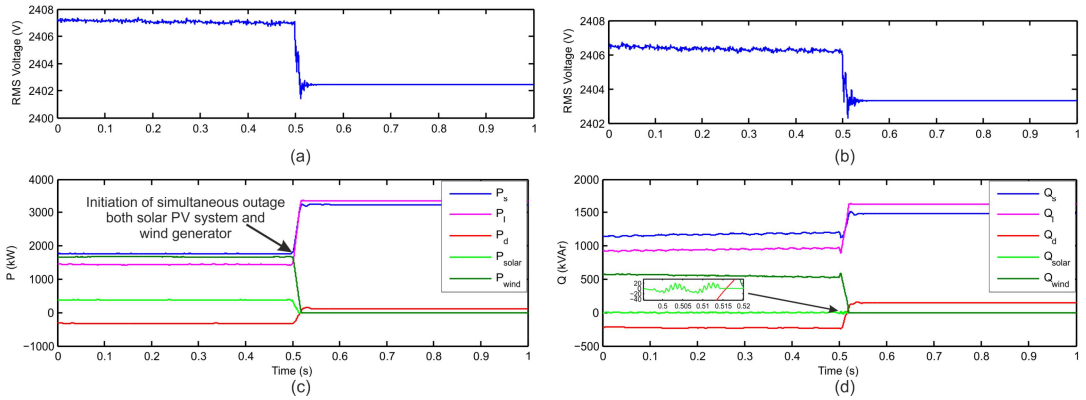

Figure 6.18 : Simultaneous outage of solar PV system and wind generator (a) Voltage without DSTATCOM (b) Voltage in the presence of DSTATCOM (c) Active powers flow with DSTATCOM and (d) Reactive powers flow with DSTATCOM

The FFT analysis of voltage signal at bus 632 is carried out. The THD_v without the use of DSTATCOM is observed as 0.1078%. The use of DSTATCOM reduced the THD_v to 0.0431%. Thus, an improvement of 60.02% in the value of THD_v has been achieved by the use of DSTATCOM with simultaneous outage of solar PV system and wind generator.

(d) Grid Synchronization of Wind Generator in the Presence of Solar PV System

The circuit breaker used to integrate wind generator is switched on at 0.5 s to simulate the grid synchronization of wind generator with solar PV system integrated to the test system. Fig. 6.19 (a) and (b) represent the voltages at bus 632 without and with DSTATCOM respectively. The active and reactive powers flow with DSTATCOM are shown in Fig. 6.19 (c) and (d) respectively. It can be observed that the voltage due to wind penetration increases followed by a voltage sag. However, in the presence of DSTATCOM voltage is slightly reduced which indicates that the voltage profile improves in the presence of DSTATCOM with BESS. This is caused due to the capacitive reactive power compensation available with the DFIG. Active and reactive powers injected by the utility grid into the test system are reduced due to the available local wind generation. The surplus active and reactive powers are absorbed by the DSTATCOM to store energy in the BESS and charging of the dc-link capacitor. High magnitude power transients are observed in the active and reactive powers for a duration of 1.2 s as depicted in Fig. 6.19 (c) and (d) respectively due to inrush current drawn by the DFIG. In the absence of DSTATCOM these transients persists for a period of 3 s (approximately). Hence, dynamic stability of the system is improved by the use of DSTATCOM.

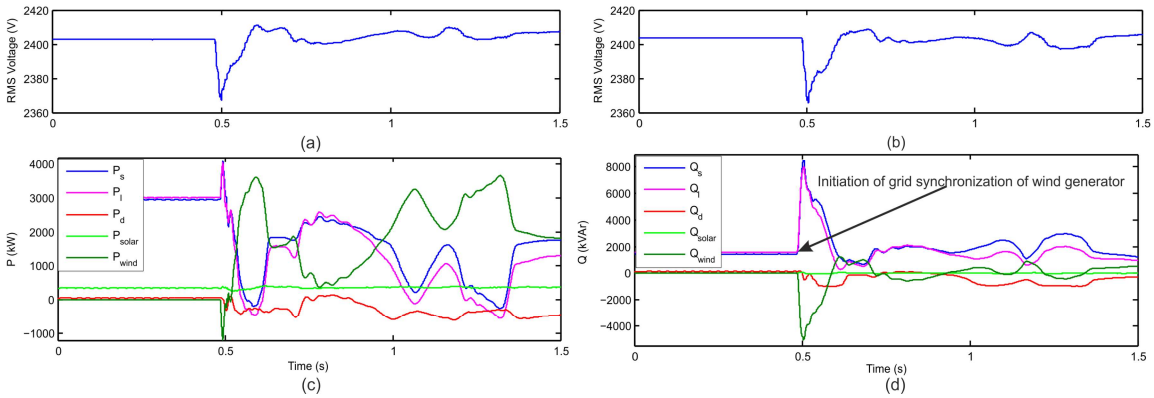

Figure 6.19 : Grid synchronization of wind generator (a) Voltage without DSTATCOM (b) Voltage in the presence of DSTATCOM (c) Active powers flow with DSTATCOM and (d) Reactive powers flow with DSTATCOM

The FFT analysis of voltage signal at bus 632 is carried out. The THD_v in the absence of DSTATCOM is observed as 0.2198%. The use of DSTATCOM has reduced the THD_v to 0.1304%. Hence, an improvement of 40.67% in the THD_v value has been achieved by the use of DSTATCOM with simultaneous outage of solar PV system and wind generator.

(e) Grid Synchronization of Solar PV System in the Presence of Wind Generator

FFT analysis of voltage signal at bus 632 is carried out. THD_v of bus voltage in the absence of DSTATCOM is observed as 0.2992%, whereas it is observed as 0.1528% in the presence of DSTATCOM with BESS. Thus, a reduction in the value of THD_v by 48.93% with the use of DTSTACOM is achieved in the event of grid synchronization of solar PV system in the presence of wind power generation.

(f) Simultaneous Grid Synchronization of Solar PV and Wind Generators

The FFT analysis of voltage signal at bus 632 is carried out. The THD_v in the absence of DSTATCOM is observed as 0.1565%. The use of DSTATCOM has reduced the THD_v to 0.0735%. Hence, an improvement of 53.04% in the value of THD_v has been achieved by the use of DSTATCOM with simultaneous outage of solar PV system and wind generator. The comparative study of THD_v with wind energy penetration is provided in Table 6.4. It can be observed that DSTATCOM

is highly effective in reduction of harmonics due to penetration of wind and solar energies into the distribution utility network.

Table 6.4 : THD of Voltage in Hybrid Power System with Wind and Solar Energies Penetration

Case studies	THD_v (%) at bus 632		Improvement in THD_v (%)
	Without DSTATCOM	With DSTATCOM	
Outage of wind generator in the presence of solar PV system	0.3192	0.1608	49.62
Outage of solar PV system in the presence of wind energy	0.2565	0.1318	48.62
Simultaneous outage of wind generator and solar PV system	0.1078	0.0431	60.02
Grid synchronization of wind generator in the presence of solar PV system	0.2198	0.1304	40.67
Grid synchronization of solar PV system in the presence of wind energy	0.2992	0.1528	48.93
Simultaneous grid synchronization of wind generator and solar PV system	0.1565	0.0735	53.04

6.7 TESTING OF RESULTS IN REAL TIME USING RTDS

Testing of the results in real time has been carried out on the real time digital simulator of OPAL-RT described in the Section 3.11. The comparison of real time results with the simulation results has been carried out in terms of THD_v and an error between simulation results and real time results is obtained. The percentage deviation (PD) of real time results from the simulation results is carried out using the relation of equation (3.11). Comparison of real time and simulation results are detailed in the following subsections.

6.7.1 Grid Disturbances

The real time results of active power flow with feeder tripping and re-closing in the presence of DSTATCOM are illustrated in Fig. 6.20. These results are very close to their respective simulation results.

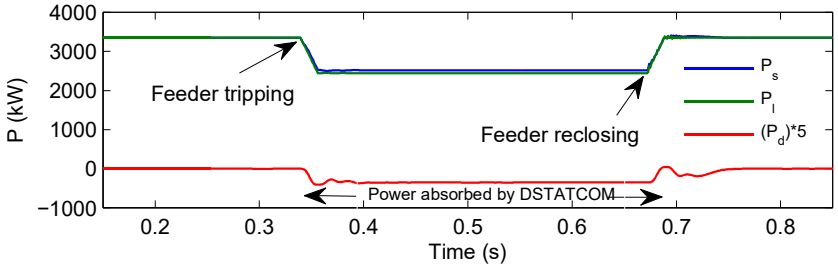

Figure 6.20 : Real time results of active power flow with feeder tripping and re-closing in the presence of DSTATCOM

The THDv of bus voltage in the presence of DSTATCOM using RTDS are obtained for all the cases of grid disturbances under study. It has been observed that real time results are very close to the simulation results. Percentage error in the value of THDv is below 1% for grid disturbances.

Therefore, the SRF theory based control of DSTATCOM has been proved to be effective for PQ improvement at grid level during the conditions of grid disturbances.

6.7.2 Wind Energy Penetration

Real time results of the active power flow with outage of wind generator in the presence of DSTATCOM are shown in Fig. 6.21. These results are very close to their respective simulation results.

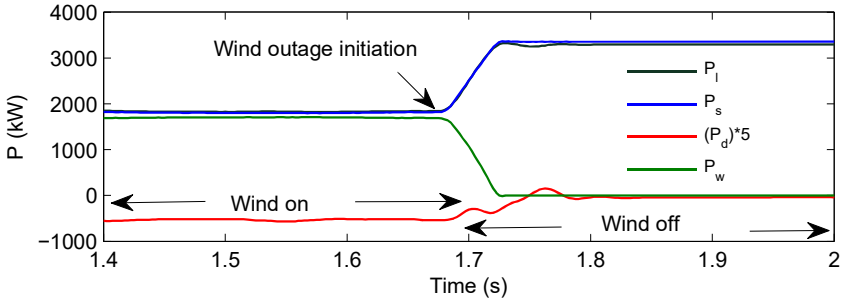

Figure 6.21 : Real time results of active power flow with wind generator outage in the presence of DSTATCOM

The THDv of bus voltage in the presence of DSTATCOM using RTDS are obtained for all cases under study of the wind energy. It can be observed that real time results are very close to the simulation results. The percentage error in the value of THDv is below 3% for the wind generator operations and wind speed variations. Therefore, the SRF theory based control of DSTATCOM has been proved to be effective for PQ improvement at grid level in the presence of wind power generation.

6.7.3 Solar Energy Penetration

Real time results of the active powers flow with outage of solar PV system in the presence of DSTATCOM with BESS are shown in Fig. 6.22. These results are very close to their respective simulation results. Hence, proposed DSTATCOM can be implemented for the power quality improvement and compensation of active and reactive powers in the distribution network.

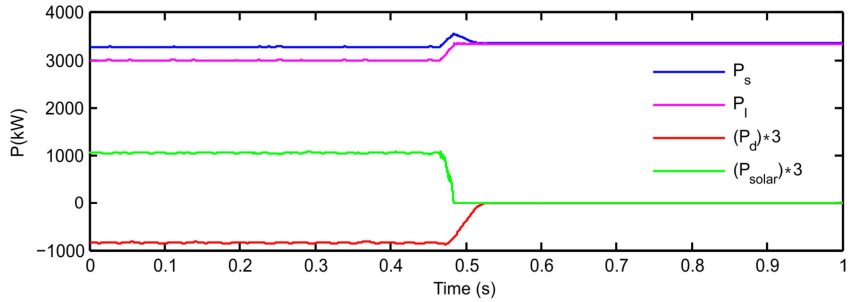

Figure 6.22 : Real time results of active power flow with outage of solar PV system in the presence of DSTATCOM

The THDv of voltage at bus 632 is obtained for all case studies using RTDS in the presence of DSTATCOM with BESS. The comparison of real time results with the simulation results in the presence of DSTATCOM with BESS has been carried out. It has been observed that real time results are very close to the simulation results. The percentage error in the value of THDv is below 1%

for outage of solar PV system and sudden change in solar insolation whereas this error is below 2% for the grid synchronization of solar PV system. Therefore, the SRF theory based control of DSTATCOM with BESS has been proved to be effective for improvement of power quality at grid level with solar energy penetration during the events such as grid synchronization and outage of solar PV system as well as sudden change in solar insolation.

6.7.4 Hybrid Power System

Real time results of the active powers flow in the event of outage of wind generator in the presence of solar PV system with DSTATCOM are shown in Fig. 6.23. These results are very close to their respective simulation results. Hence, proposed DSTATCOM can be implemented for the power quality improvement and compensation of active and reactive powers in the distribution utility network.

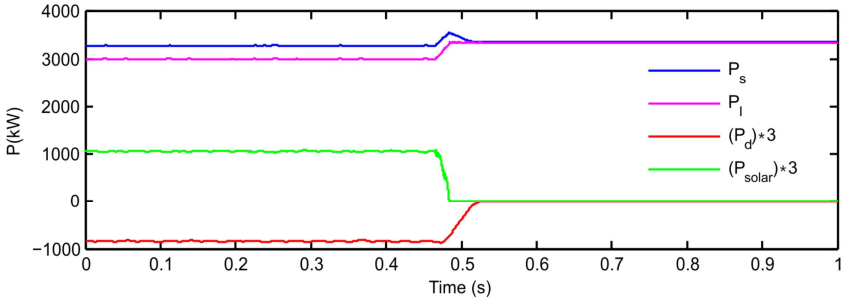

Figure 6.23 : Real time results of active power flow with outage of solar PV system in hybrid power system with DSTATCOM

THDv of voltage at bus 632 is obtained for all case studies using RTDS in the presence of DSTATCOM with BESS. It has been observed that real time results are very close to the simulation results. Percentage error in the value of THDv is below 1% for all outage events whereas this error is below 2% for all synchronization events. Therefore, the SRF theory based control of DSTATCOM with BESS has been proved to be effective for improvement of power quality at grid level in hybrid power system with wind and solar PV integration during the events of grid synchronization and outage of wind generator and solar PV system.

6.8 CONCLUSIONS

The research work presented in this chapter is related to mitigation of PQ events associated with distribution network integrated with wind generator and solar PV system. The DSTATCOM with BESS has been proposed to improve the power quality in the events of grid disturbances such as voltage sag, swell, load switching, feeder tripping and re-closing. Power quality events associated with wind operations such as wind generator outage, grid synchronization of wind generator and wind speed variations have been improved by the use of proposed DSTATCOM in the distribution network. The DSTATCOM is also utilized to improve the power quality events associated with the operations of solar PV system such as grid synchronization, outage of the solar PV system and sudden change in solar insolation. The proposed DSTATCOM with battery energy storage system is also effectively applied to improve power quality in the events of grid synchronization and outage of wind generator and solar PV system as well as simultaneous operations of these generators in hybrid power system. The proposed DSTATCOM with SRF theory based control has been proved to be effective in improving the power quality in these events at grid level. From, these studies it has been established that DSTATCOM with BESS can effectively be used to im-

prove the power quality in the distribution network with wind generation, solar PV generation, hybrid power system and during grid disturbances. The results have been tested in real time using RTDS. Real time results are very close to the simulation results which shows the effectiveness of proposed DSTATCOM with BESS for improvement of PQ in the distribution system.

…